Department of Pharmaceutical Technology, Anadolu University, Eskisehir, Turkey

Solid lipid nanoparticles: A possible vehicle for zinc oxide and octocrylene

M. S. Berkman, Y. Yazan

Received July 7, 2011, accepted August 10, 2011

Assist. Prof. Murat Sami Berkman, Faculty of Pharmacy, Department of Pharmaceutical Technology, Anadolu University, 26470, Eskisehir, Türkiye
muratsb@anadolu.edu.tr

Pharmazie 67: 202–208 (2012) *doi: 10.1691/ph.2012.1098*

An efficient sunscreen formulation shows good absorption in the relevant UV range. Efficacy also means that the UV absorber must be easily incorporated in any kind of formulation. In this study, a chemical absorber, octocrylene, and one of the most important physical blockers, zinc oxide, could be successfully incorporated into Solid Lipid Nanoparticle (SLN) systems which themselves have UV blocking potential similar to physical sunscreens, and remained stable for a period of 360 days while providing UVA and UVB protection. Crystalline structure related to the chemical nature of the solid lipid is a key factor to decide whether a sunscreening agent will be expelled or incorporated in the long-term and for a controlled optimization of active ingredient incorporation and loading, intensive characterization of the physical state of the lipid particles was highly essential. Thus, FT-IR, NMR, XRD and DSC analyses were performed and the results did not indicate stability problems. pH values of the SLN systems were found to be between 5.4–5.9 in all formulations which may be buffered by the skin. Transpore^{TM} test results proved the UV blocking potential of the SLNs with not any active ingredient and the synergistic effects by the incorporation of molecular sunscreens. Therefore, concentration of molecular sunscreens in the formulations was decreased to 0.6%. UVA and UVB screening potentials of octocrylene and zinc oxide formulations were compared in the 290–400 nm wavelength region. Zinc oxide loaded SLN suspensions were found to be more effective in the UVA region while octocrylene loaded ones performed better in the UVB region.

1. Introduction

A sunscreen product is any preparation (e.g. cream, oil, gel, spray) intended to be placed in contact with human skin with the exclusive or main objective being the protection of the skin from harmful UV radiation through absorption, scattering or reflection (Cf. Art. 1 of the draft “Recommendation on efficacy and claims relating to sunscreen products”). UV filters are traditionally classified as chemical absorbers or physical blockers depending on their mechanism of action. Sunscreens provide UV protection either by incorporating chemical absorber (absorbing) or physical blocker (scattering and reflecting) materials (Poiger et al. 2004; Simeoni et al. 2005).

The conventionally accepted spectral limits of UV radiation are 320–400 nm for UVA, 290–320 nm for UVB and 200–290 nm for the UVC region (Herzog et al. 2004; Levy 2009). UVC is filtered by the ozone layer in the atmosphere before reaching the surface of the earth and therefore plays a minor role in natural photochemical reactions. UVB is responsible for the damage incurred by sunburn. UVA reaches the deeper layers of the epidermis and dermis, but is also emitted from artificial lamps. In order to provide an adequate sun protection factor (SPF), it is necessary to combine agents with a wide range of UV protection properties (Azevedo et al. 1999). An ideal sunscreen should have broad-spectrum protection along the entire range of UVA and UVB spectra. Efficacy of sunscreens depends on their UV absorption, concentration, formulation and the ability to withstand liquid contact such as swimming or perspiration.

Due to their lipidic and particulate character, SLNs act as physical sunscreens when empty. Incorporation of molecular sunscreens is possible and leads to long-term stable formulations and synergistic UV-blocking effects (Wissing and Müller 2003; Demirel and Yazan 2000). Therefore, the concentration of molecular sunscreens in a formulation can be decreased while maintaining the same protection level (Wissing and Müller 2001).

In this study, a chemical absorber, octocrylene (2-ethylhexyl-2-cyano-3,3-diphenylacrylate) and a physical blocker, zinc oxide, were incorporated into SLN systems and the UV-blocking capacities of loaded and empty SLN suspensions were investigated. Octocrylene (OCR) is a UVB absorber while zinc oxide is effective in both UVA and UVB regions (Anderson et al. 1997). The approved application level of octocrylene is up to 10% alone and 7–10% when used in combination with other sunscreening agents (Salvador and Chisvert 2005). Zinc oxide (ZnO) has an application range of 20–25% in sunscreening formulations (Anderson et al. 1997).

2. Investigations, results and discussion

2.1. *Characterization of SLN formulations*

Different particle shapes of SLNs were observed in various studies (Demirel et al. 2001; El-Gibaly and Abdel-Ghaffar 2005). Some of them were uniform and spherical in shape while some were amorphous and irregular as in this study (Bodmeier et al. 1991; Wissing et al. 2004). The preparation method and the

Table 1: Mean particle size and distribution of OCR and ZnO loaded SLNs

		OCR			ZnO	
Storage condition	Codes	Mean ± SE (nm)	PDI ± SE	Codes	Mean ± SE (nm)	PDI ± SE
25 °C	FSO-T0	117.0 ± 1.5	0.243 ± 0.044	FSZ-T0	102.0 ± 1.4	0.366 ± 0.043
	FSO-T15	119.0 ± 1.2	0.241 ± 0.016	FSZ-T15	113.0 ± 1.0	0.415 ± 0.036
	FSO-T30	124.0 ± 0.8	0.248 ± 0.058	TSZ-T30	103.0 ± 1.3	0.310 ± 0.064
	FSO-T90	122.0 ± 1.3	0.224 ± 0.088	FSZ-T90	100.0 ± 1.0	0.232 ± 0.052
	FSO-T180	139.0 ± 0.9	0.145 ± 0.084	FSZ-T180	122.0 ± 1.2	0.157 ± 0.085
	FSO-T360	143.0 ± 1.4	0.168 ± 0.060	FSZ-T360	148.0 ± 1.1	0.149 ± 0.054
4 °C	FSO-T0	117.0 ± 1.5	0.243 ± 0.044	FSZ-T0	102.0 ± 1.4	0.366 ± 0.043
	FSO-T15	125.0 ± 1.2	0.257 ± 0.018	FSZ-T15	112.0 ± 1.4	0.342 ± 0.076
	FSO-T30	136.0 ± 1.4	0.305 ± 0.011	FSZ-T30	110.0 ± 1.0	0.350 ± 0.068
	FSO-T90	123.0 ± 1.1	0.251 ± 0.037	FSZ-T90	117.0 ± 1.1	0.442 ± 0.062
	FSO-T180	126.0 ± 1.1	0.264 ± 0.040	FSZ-T180	129.0 ± 1.0	0.421 ± 0.012
	FSO-T360	185.0 ± 0.8	0.279 ± 0.023	FSZ-T360	162.0 ± 1.0	0.529 ± 0.076
40 °C	FSO-T0	117.0 ± 1.5	0.243 ± 0.044	FSZ-T0	102.0 ± 1.4	0.366 ± 0.043
	FSO-T15	127.0 ± 1.2	0.190 ± 0.017	FSZ-T15	109.0 ± 1.1	0.279 ± 0.087
	FSO-T30	194.0 ± 1.2	0.289 ± 0.032	FSZ-T30	114.0 ± 1.4	0.202 ± 0.089
	FSO-T90	517.0 ± 1.0	0.268 ± 0.013	FSZ-T90	181.0 ± 1.1	0.339 ± 0.038
	FSO-T180	681.0 ± 1.1	0.336 ± 0.078	FSZ-T180	1370.0 ± 1.0	0.389 ± 0.076
	FSO-T360	698.0 ± 1.1	0.344 ± 0.059	FSZ-T360	1398.0 ± 1.0	0.985 ± 0.028

$n = 3$ SE: standard error PDI: polydispersity index

preferred carrier system were reported to have a significant effect on the particle shapes. Gel formation was observed on the samples stored at 40 °C after 360 days while the others remained stable and furthermore, no sedimentation was observed upon centrifugation studies.

pH values of OCR and ZnO loaded SLNs on the 15th, 30th, 90th, 180th and 360th days were determined and changed only slightly between 5.4 and 5.9. Minor pH changes seen in the figures may be due to the deficiency of the buffer system, change in the particles surface, unstabilization of the active ingredient or microbiological growth (Acartürk 2007). However, no significant changes were detected in pH values upon statistical evaluation ($p > 0.05$). Based on these findings, it can be said that the formulations are stable during the storage period of 360 days.

Particle size is one of the most important physical properties of colloidal carrier systems. The particle size distribution of the formulation is especially significant in the physical stability and activity of colloidal systems such as suspensions and emulsions (Takka et al. 2007). In a study where the relationship between storage conditions and gel formation at high temperatures, light or any energy input such as kinetic energy was examined, it was observed that these factors increase the possibility of gelatinization (Freitas et al. 2007). Increase in the mean particle size of the SLN formulations after 360 days can be explained as a stability problem and/or formation of aggregates due to storage conditions. Since free energy on the small particles is greater than the bigger particles, small particles may be crystallized and transformed into larger particles. Polymorphism, simultaneous use of crystal and amorphous structures, temperature changes and excessive amounts of surfactants used may also be the reason for crystal growth (Takka et al. 2007). Polydispersity indices (Table 1) of the SLN formulations prepared in this study were low, approximately 0.300, which indicates homogeneous distribution.

Zeta potential measurements of the SLN formulations provide information about the storage stability of colloidal dispersions (Kaş 2004). In general, systems with a high zeta potential values are more resistant to aggregate formation (Müller et al. 2000). Systems that have an electrical conductivity in the range of -31 to -60 mV have moderate, -61 to -80 mV have fine and -81 to −100 mV have excellent electrostatic stability (Müller and Heinemann 1993). Changes in the zeta potentials of SLN formulations may be caused by formation of aggregates due to storage conditions and/or stability problems. Zeta potential and electrical conductivity values of OCR and ZnO loaded SLNs on the 15th, 30th, 90th, 180th and 360th days are presented in Figs. 1–4 respectively. Each figure provides an associated comparison.

When performing the thermal analyses with differential scanning calorimeter (DSC) on the lyophilized formulations, two peaks were observed, one for the melting and one for the freezing

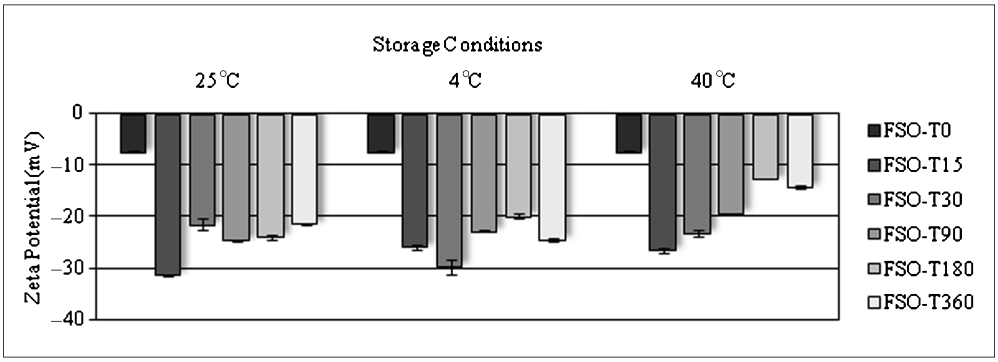

Fig. 1: Zeta potentials of OCR loaded SLNs (n = 3)

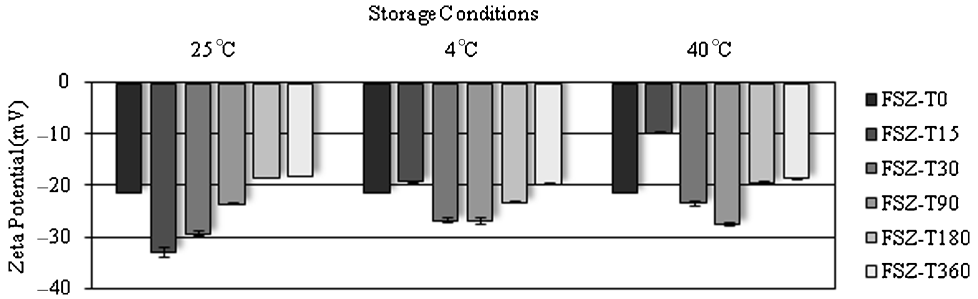

Fig. 2: Zeta potentials of ZnO loaded SLNs (n = 3)

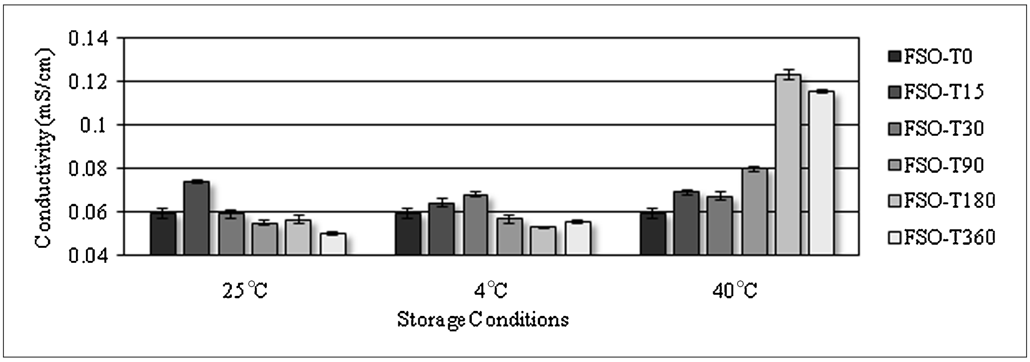

Fig. 3: Electrical conductivities of OCR loaded SLNs (n = 3)

repectively. Crystallization of the lipid in nanoparticles is different to the bulk material, lipid nanoparticles recrystallize at least partially in the α-form, whereas bulk lipids tend to recrystallize preferentially in the β'-modification and transforming rapidly into the β-form. Therefore the melting point of Dynasan® 116 was found to be 63 °C while the SLN formulations was approximately 61 °C and still having a similar peak geometry during the storage conditions. Thermal analyses results of the SLNs stored at 25 °C, 4 °C and 40 °C are shown in Table 2.

For the investigation of molecular structure and polymorphism of SLNs x-ray diffractometer (XRD) was used and the characteristic peak of Dynasan® 116 at 18.95 (2θ) and the triple peak of ZnO at 32, 34 and 36 (2θ) were confirmed in all formulations. When the X-ray profiles are analyzed data not shown, there was no movement or deformation in the bands and it can be concluded that all the formulations remained stable after 360 days. XRD analysis of OCR failed because of its liquid form.

SLN formulations were compared with the freshly prepared formulations, Dynasan® 116 and OCR by fourier transform infrared (FT-IR) spectroscopy. Neither movement or deformation in the bands nor any stability problems were observed. When FT-IR data were analyzed, the formulations remained stable for 360 days. However, on the 360th day, FT-IR spectrum of ZnO loaded SLNs at 40 °C showed that the intensity of the characteristic band (C = O ester at 1780 cm^{-1}) of the solid lipid was lower than the freshly prepared formulations. This was interpreted as the breaking of the Dynasan® 116 ester structure and the formation of the acidic carbonyl group. Such degradation would explain why the pH of the formulations is decreasing. Furthermore, nuclear magnetic resonance (NMR) spectra of SLNs were compared to those of the freshly prepared samples, Dynasan® 116 and OCR. Characteristic 10 aromatic protons in OCR were observed as multiple peaks at about 7 ppm. NMR analysis of OCR failed due to its molecular structure. ZnO and OCR formulations were evaluated separately. Movement or deformation in the bands and stability problems were not observed. NMR data showed that the formulations remained stable after 360 days.

2.2. *Determination of OCR*

Linearity equation of OCR was calculated to be $y = 14533x + 0.0032$ ($r^2 = 0.9977$) by HPLC (Berkman and Yazan 2011). Limit of detection (LOD) and limit of quantitation (LOQ) values were 1.64×10^{-6} M and 4.97×10^{-6} M, respectively. Free, superficial and loaded quantities of OCR in the SLN sus-

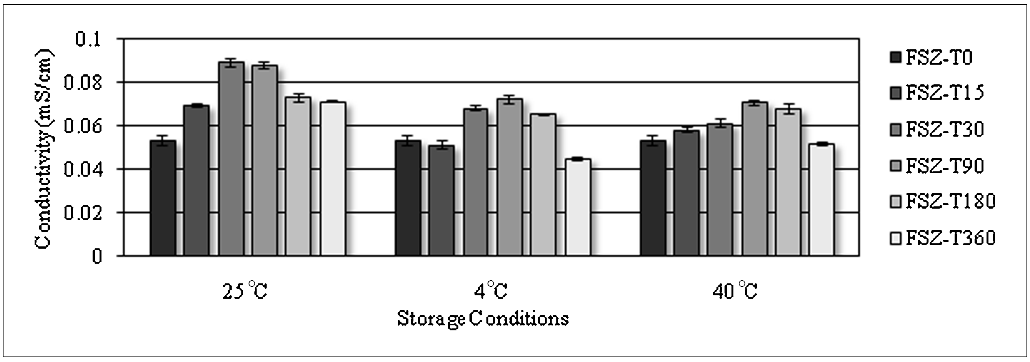

Fig. 4: Electrical conductivities of ZnO loaded SLNs (n = 3)

Table 2: Thermal analysis results of OCR and ZnO loaded SLNs

Storage condition	Codes	OCR				Codes	ZnO			
		Melting		Freezing			Melting		Freezing	
		Temp (°C)	Heat (J.g^{-1})	Temp (°C)	Heat (J.g^{-1})		Temp (°C)	Heat (J.g^{-1})	Temp (°C)	Heat (J.g^{-1})
25 °C	FSO-T0	61.91	−57.92	39.46	35.81	FSZ-T0	62.52	−81.00	40.82	50.19
	FSO-T15	60.94	−63.56	39.74	36.29	FSZ-T15	62.51	−76.32	40.83	47.00
	FSO-T30	62.45	−75.78	39.09	46.72	FSZ-T30	62.76	−82.61	40.66	49.71
	FSO-T90	61.42	−78.10	39.45	48.33	FSZ-T90	62.40	−81.56	40.68	50.28
	FSO-T180	61.93	−75.82	39.35	46.97	FSZ-T180	61.85	−92.20	41.10	54.10
	FSO-T360	61.43	−68.84	39.71	45.43	FSZ-T360	61.73	−89.13	41.14	52.49
4 °C	FSO-T0	61.91	−57.92	39.46	35.81	FSZ-T0	62.52	−81.00	40.82	50.19
	FSO-T15	61.87	−72.92	39.42	43.37	FSZ-T15	62.21	−82.40	40.98	49.92
	FSO-T30	62.01	−88.68	39.47	51.55	FSZ-T30	61.82	−62.44	40.98	37.98
	FSO-T90	61.42	−84.24	39.55	51.13	FSZ-T90	61.94	−80.97	40.94	47.56
	FSO-T180	61.65	−81.74	39.76	46.31	FSZ-T180	62.35	−87.64	41.06	53.38
	FSO-T360	61.72	−82.53	39.44	48.36	FSZ-T360	61.84	−84.35	40.88	55.45
40 °C	FSO-T0	61.91	−57.92	39.46	35.81	FSZ-T0	62.52	−81.00	40.82	50.19
	FSO-T15	60.62	−100.68	38.00	62.99	FSZ-T15	61.55	−83.74	39.65	52.64
	FSO-T30	60.64	−87.91	38.09	57.28	FSZ-T30	61.77	−99.30	39.61	60.49
	FSO-T90	61.06	−73.29	37.72	47.49	FSZ-T90	62.21	−89.10	39.39	54.01
	FSO-T180	60.71	−82.27	38.05	51.55	FSZ-T180	61.85	−85.18	38.97	53.57
	FSO-T360	60.64	−86.36	37.99	58.25	FSZ-T360	61.94	−84.26	39.25	52.88

pensions and % recovered, SE, RSD and 95% CI values are given in Table 3.

The final SLN formulation consisted of 6% solid lipid and the active ingredient (10% of the solid lipid mass). Free, superficial and loaded amounts of the active ingredient were 2.47%, 87.15% and 9.36%, respectively. Total recovery % was found to be 98.98% for the freshly prepared SLNs. The 1.02% loss in active ingredient may be due to any sticking to the beaker or stirrer during the preparation stage.

After a 360-day storage period, the free OCR quantity increased from 2.47% to 3.22% (25 °C), 3.23% (4 °C) and 7.37% (40 °C). This may be due to the slow transfer of the superfacial active ingredient to the aqueous phase.

The superfacial OCR quantity of 87.15% decreased to 79.54% (25 °C), 78.73% (4 °C) and 72.15% (40 °C) after a 360-day storage period. The reason of this decrease may be the aforementioned slow transfer of the active ingredients to the aqueous phase or any stability problem.

OCR quantity loaded was found to be 9.36%. After a 360-day storage period the quantity changed to 9.06% (25 °C), 8.74% (4 °C) and 6.19% (40 °C) which may be due to the transfer of the active ingredient through the phases or stability problems.

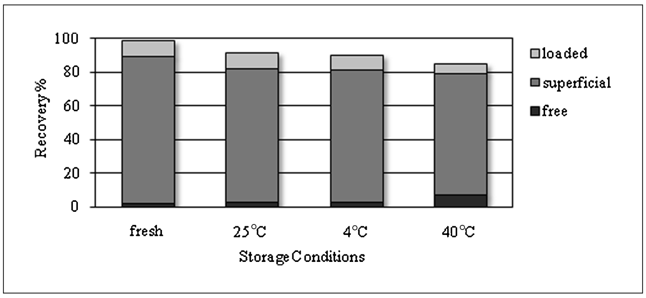

Fig. 5: Recovery % of OCR from SLNs

OCR recovery % results of the SLN formulations stored at 25 °C, 4 °C and 40 °C for 360 days were compared to the freshly prepared samples and demonstrated in Fig. 5.

2.3. *Determination of ZnO*

Linearity equation of ZnO was calculated to be $y = 59.985x + 20.517$ ($r^2 = 0.9999$) by inductively coupled plasma optical emission spectrometry (ICP-OES). SE, RSD and 95% CI values of the optical emission spectroscopy used are shown in Table 4.

Table 3: Recovery % of OCR from SLNs

	Codes		Recovery % ± SE	RSD	CI 95%
	FSO-T0		2.47 ± 0.01	1.15	± 0.03
Free	FSO-T360	4 °C	3.23 ± 0.01	0.60	± 0.02
	FSO-T360	25 °C	3.22 ± 0.02	1.19	± 0.04
	FSO-T360	40 °C	7.37 ± 0.02	0.77	± 0.06
	FSO-T0		87.15 ± 0.17	0.49	± 0.45
Superficial	FSO-T360	4 °C	78.73 ± 0.20	0.64	± 0.52
	FSO-T360	25 °C	79.54 ± 0.21	0.66	± 0.55
	FSO-T360	40 °C	72.15 ± 0.25	0.86	± 0.66
	FSO-T0		9.36 ± 0.24	6.23	± 0.61
Loaded	FSO-T360	4 °C	8.74 ± 0.35	9.95	± 0.91
	FSO-T360	25 °C	9.06 ± 0.32	8.74	± 0.83
	FSO-T360	40 °C	6.19 ± 0.35	13.77	± 0.89

$n = 6$ SE: standard error RSD: relative standard deviation CI: confidence interval

Table 4: Recovery % of ZnO from SLNs

Codes		Recovery % ± SE	RSD	CI 95%
FSZ-T0		96.18 ± 0.24	0.43	± 1.0325
FSZ-T360	4 °C	97.15 ± 0.50	0.89	± 2.1594
FSZ-T360	25 °C	87.45 ± 0.65	1.29	± 2.7995
FSZ-T360	40 °C	87.61 ± 0.34	0.68	± 1.4764

n = 3 SE: standard error RSD: relative standard deviation CI: confidence interval

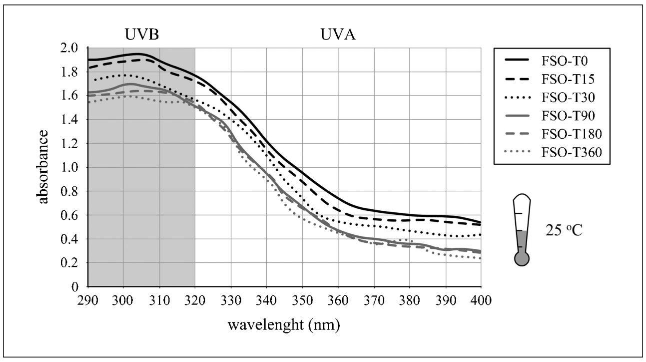

Fig. 6: Comparison of freshly prepared OCR loaded SLNs using Transpore™ test on 15th, 30th, 90th, 180th and 360th days at 25 °C

Total recovery % was found to be 96.18%. The reason for the 3.82% loss in the active ingredient may be sticking to the beaker and stirrer during the preparation stage.

Regarding ZnO, there were no stability problems or weight losses; hence only the amount of ZnO when stored at 25 °C, 4 °C and 40 °C were calculated after a 360-day period. These results allowed the determination of the amount of ZnO which can be loaded into the system.

2.4. *Transpore™ test*

UV protection abilities of the SLN formulations investigated by the *in vitro* Transpore™ test method provided comparison of the formulations (Figs. 6–7). Profiles on the 15th, 30th, 90th, 180th and 360th days displayed insignificant differences while the difference was found to be significant between OCR and ZnO formulations. Even though the same amount of active ingredient was loaded to the systems, UV blocking efficacy of the chemical absorber OCR was found to be much better than the physical blocker ZnO. UV absorbances of the ZnO loaded SLN formulations were between 0.4–0.7 while OCR loaded SLN formulations showed up to 2.0 absorbance in the UVB region. However, the UVA filtering potential of ZnO loaded SLNs was better than OCR loaded SLNs when the formulations were compared in the 360–400 nm wavelength region (Kullavanijaya and Lim 2005). For the demonstration of synergistic UV-blocking effects, FSE, OCR and ZnO were compared in Fig. 8, by only mixing an oil (capric/caprylic triglyceride) with these two sunscreen agents.

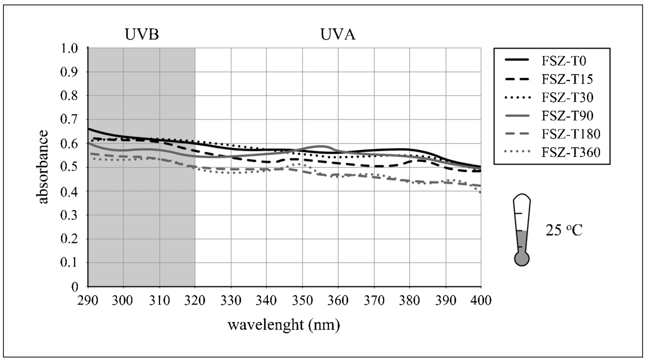

Fig. 7: Comparison of freshly prepared ZnO loaded SLNs using Transpore™ test on 15th, 30th, 90th, 180th and 360th days at 25 °C

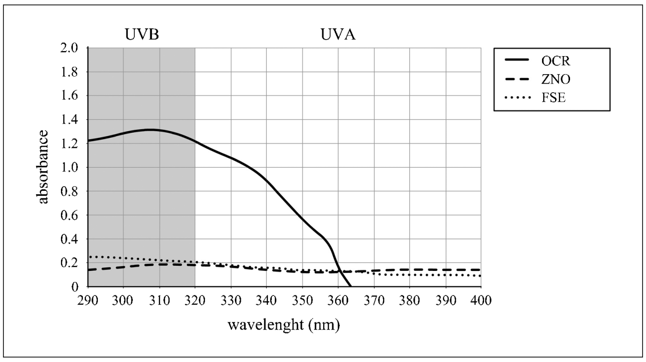

Fig. 8: Transpore™ test result of empty SLN formulation

3. Experimental

3.1. *Materials*

UV filter octocrylene (Eusolex® OCR) was provided by Merck KgaA (Germany) and zinc oxide from Carlo Erba Reactifs SA (France). Solid lipid tripalmitin (Dynasan® 116) was purchased from Fluka Chemie GmbH (Switzerland) and the surfactant polyoxyethylene sorbitan monooleat (Tween® 80) from Merck Schuchardt (Germany). Deuterated chloroform used for NMR spectroscopy analysis and the mobile phase, analytical-reagent grade acetonitrile for the high performance liquid chromatography were purchased from Merck KgaA (Germany) and used with no purification. The internal standard cyclosporine A was supplied by Novartis (Türkiye). Transparent tapes for Transpore™ Test were provided by 3 M (USA).

3.2. *Preparation of nanoparticles*

The melting point measurements of Dynasan® 116 were conducted using a basic melting point device (Electrothermal 9100, USA) with capillary tubes and a differential scanning calorimeter (Shimadzu DSC 60, Japan). Measurements were repeated 3 times and the average melting point was found to be 63 °C. For empty formulations, the hot aqueous surfactant solution was dispersed in the molten solid lipid at elevated temperatures and stirred by a high-performance dispersing instrument to get a hot oil-in-water emulsion. Speed range was varied between 3–5 min. at 8000–13500 rpm using an ultraturrax (Janke&Kunkel® IKA, Labortechnik, Germany). In order to prepare nanoparticles by hot emulsion method, the lipid phase was melted at 10 ± 1 °C above the melting point of the solid lipid and the temperature was set at 73 ± 1 °C in a thermostated water bath during the stirring (Scalia and Mezzena 2009). 20 g of nanoemulsion pre-mixtures prepared in 50 mL small glass beakers were then isolated from external effects and cooled down to room temperature. SLNs were formed after recrystallization. Following the optimization of empty formulations, OCR and ZnO -10% of the solid lipid mass- were dispersed in the molten lipid phase and the procedure mentioned above was applied. Different ratios of the solid lipid (5–20 %) and the surfactant (1–5 %) were used to investigate their effects on particle size distribution. These pre-mixtures were then homogenized using a high pressure homogenizer APV-2000 (Denmark) applying three homogenization cycles at 500 bar. Lyophilization process was applied to the formulations prepared using a Leybold-Heraeus Lyovac GT–2 (Germany). Table 5 provides an overview of the final SLN formulations selected.

3.3. *Characterization of nanoparticles*

SLNs were stored at 25 ± 0.1 °C (room temperature), 4 ± 0.1 °C and 40 ± 0.1 °C in small glass vials over a period of 12 months to observe their physical properties. Stability tests were repeated on the 15th, 30th, 90th, 180th and 360th days and UV protection abilities of the formulations were investigated and compared using *in vitro* Transpore™ Test method (Cengiz et al. 2006). Codes of the SLN formulations used during the characterization studies are presented in Table 6. SLNs lyophilized were placed on a carbon tape and coated with gold atoms under an argon atmosphere and the surface characteristics of the formulations were investigated using a scanning electron microscope (SEM) (FESEM SUPRATM 50 VP ZEISS, Germany). Any changes in the visual appearances of the samples were examined. Fur-

Table 5: Dynasan® 116-based SLN formulations

	Empty Formulation	OCR Formulation	ZnO Formulation
Code	FSE	FSO	FSZ
Dynasan®116	6%	6%	6%
Tween® 80	4%	4%	4%
Active ingredient	–	0.6%	0.6%
Distilled water	90%	89.4%	89.4%
Stirrer	Ultraturrax	Ultraturrax	Ultraturrax
Temperature	73 °C	73 °C	73 °C
Stirring rpm	13500	13500	13500
Stirring time	5 min	5 min	5 min
Homogenization	500 bar 3 cycles	500 bar 3 cycles	500 bar 3 cycles
Particle size	100–150 nm	100–150 nm	100–150 nm

thermore, sedimentation of the SLN suspensions was forced by using a centrifuge (Jouan B4, Germany) at 1000 rpm for 5 min.

pH values of the formulations were measured using a pH-meter (WTW Profi Lab pH 597, Germany) repeating each measurement three times. Particle size distribution and zeta potential values of the formulations were determined by a Zetasizer (Nano Zetasizer ZS, Malvern Instruments, UK). The mean particle size and distribution were measured based on non-invasive back scatter (NIBS) technology, which is a powerful and versatile tool for the accurate, reliable and repeatable size analysis of particles and molecules in solution ranging from a few nanometers to several micrometers. Zeta potential is a very useful way of evaluating the stability of any colloidal system, and it was determined based on a combination of laser Doppler velocimetry and phase analysis light scattering (PALS) techniques. Analyses were performed in disposable capillary green zeta cells at 25 °C by diluting the samples. Conductivity of distilled water was adjusted to 50 µS with NaCl to avoid any conductivity changes. Measurements on each sample were repeated thrice.

Thermal analyses of the SLN formulations were performed by a DSC (Shimadzu DSC 60, Japan). 5 ± 0.1 mg lyophilized samples placed in aluminium pans were closed tightly using pressure and analyses were performed against a blank reference pan at a nitrogen gas flow rate of 200 mL·min^{-1}. The samples were heated from 25 °C to 100 °C at a heating/cooling rate of 5 K· min^{-1}.

X-ray diffractometer XRD-RIKAGU Rint 2000 (Japan) was used for the investigation of molecular structure and polymorphism of SLNs. Crystallinity of the formulations were determined between 4–40 °C at a 2°/min^{-1} scanning rate with an anode voltage of 40 kV and a current of 20 mA provided by a Rigaku generator.

SLNs were scanned in the range of 400–4000 cm^{-1} using FT-IR spectroscopy (Perkin Elmer FT-IR Spectrometer, Spektrum 2000, UK) with a KBr disc and nuclear magnetic resonance (NMR) analyses (Ultra Shield CP MAS NMR, Brucker, Germany) of the SLNs were performed using deuterated chloroform as the solvent.

3.4. Determination of OCR

HPLC (Shimadzu SPD-MID A VP, Japan) was used to determine the amount of OCR incorporated into the SLNs prepared. The “Analytical Process Validation Method of the International Harmonization Committee” (ICH Q2B 1996) was used for method validation and the linearity, accuracy, precision and specificity parameters were evaluated. Operating conditions of the HPLC method used are shown in Table 7.

Table 6: Codes of the SLN formulations prepared

FSO-T0	freshly prepared OCR loaded SLN
FSO-T15	OCR loaded SLN after 15-day storage
FSO-T30	OCR loaded SLN after 30-day storage
FSO-T90	OCR loaded SLN after 90-day storage
FSO-T180	OCR loaded SLN after 180-day storage
FSO-T360	OCR loaded SLN after 360-day storage
FSZ-T0	freshly prepared ZnO loaded SLN
FSZ-T15	ZnO loaded SLN after 15-day storage
FSZ-T30	ZnO loaded SLN after 30-day storage
FSZ-T90	ZnO loaded SLN after 90-day storage
FSZ-T180	ZnO loaded SLN after 180-day storage
FSZ-T360	ZnO loaded SLN after 360-day storage

Table 7: Operating conditions of HPLC

Mobile phase	Acetonitrile:water (75:25, v/v)
Injection volume	20 µL
Oven temperature	50 °C
Flow rate	1.5 mL min^{-1}
Column	4.6 × 250 mm, 5 µm C_{18} ACE
Detection	210 nm

The external phase of the suspension was diluted with distilled water and filtered through a 0.1 µm polyamide filter in order to calculate the amount of free (in water) OCR in the SLN suspension. SLN suspension was mixed with ethanol at 25 °C to calculate the superficial OCR; mixed with ethanol at 70 °C in an ultrasonic bath for the loaded amount. Accurately weighed cyclosporine A was mixed with the mobile phase to obtain a 0.202 mg.mL-1 solution and used as the internal standard (IS) solution for each measurement. Experiments were repeated 6 times for each sample and the amount of OCR in the formulations were expressed as the % recovered. Standard error (SE), relative standard deviation (RSD) and 95% confidence interval (CI) values were also calculated.

3.5. Determination of ZnO

A formerly calibrated method by device itself was used to achieve the ZnO quantification using ICP-OES. Calibration standards were prepared using 1000 ppm standard zinc solution provided by NIST SRM (National Institute of Standards and Technology Standard Reference Materials) 3168 and the linearity of the method was evaluated. The operating conditions of the ICP-OES method are shown in Table 8.

The only inorganic substance, ZnO, in the formulation is resistant to high temperatures and has a melting point of 1975 °C. Therefore, the formulation was burned at 500 °C in an ash oven, and ZnO was seperated from the other components. Due to the solubility of ZnO in diluted acids, 5% HCl was used as the solvent and measurements were carried out using ICP-OES. Experiments were repeated 3 times for each sample and the active ingredient amounts in the formulations were expressed as % recovered. SE, RSD and 95% CI values of the results were also calculated.

Table 8: Operating conditions of ICP-OES

Detection	206.200 nm	
Source equalization	15 s	
Sample flow rate	1.5 mL min^{-1}	
Power	1450 W	
Cycle	3	
Retention time	10 s	
Plasma viewing	vertical	
	plasma	16 L min^{-1}
Torch Ar gas flow rate	auxiliary	0.2 L min^{-1}
	nebuliser	0.55 L min^{-1}

3.6. *Transpore^{TM} test*

UV protection abilities of the formulations were investigated and compared using the *in vitro* Transpore^{TM} test method (Cengiz et al. 2006). The substrate that is used for formulations is Transpore^{TM} tape which has a knobbled surface that has been found to distribute the sunscreen compounds in a way similar to the uneven topography of human *Stratum corneum*. The principle of the method is to measure the spectral transmission of UV radiation through a sample of Transpore^{TM} tape with and without the formulation applied (Diffey and Robson 1989).

Acknowledgements: AUBİBAM (Anadolu University Medicinal Plants, Drugs and Scientific Research Center) is acknowledged for the technical support in HPLC and ICP-OES studies. This research was supported by Anadolu University Scientific Research Projects Committee (Project no 040343).

References

Acartürk F, Süspansiyonlar (2007) In: Acartürk F, Ağabeyoğlu İ, Çelebi N, Değim T, Değim Z, Doğanay T, Takka S, Tırnaksız F (eds.) Modern Farmasötik Teknoloji. Ankara: Türk Eczacıları Birliği Eczacılık Akademisi Yayını, Fersa Matbaacılık Ltd Şti, pp. 301–316.

Anderson MW, Hewitt JP, Spruce SR (1997) Broad-spectrum physical sunscreens: Titanium dioxide and zinc oxide. In: Lowe NJ, Shaath NA, Pathak MA (eds) Sunscreens: Development, evaluation and regulatory aspects. New York: Marcel Dekker Inc, pp. 353–399.

Azevedo JS, Viana NS, Vianna Soares CD (1999) UVA/UVB sunscreen determination by second-order derivative ultraviolet spectrophotometry. Farmaco 54: 573–578.

Berkman MS, Yazan Y (2011) A validated HPLC method for the determination of octocrylene in solid lipid nanoparticle systems. Pharmazie 66: 105–110.

Bodmeier R, Chen H, Tyle P, Jarosz P (1991) Spontaneous formation of drug-containing acrylic nanoparticles. J Microencapsulation 8: 161–170.

Cengiz E, Wissing SA, Müller RH, Yazan Y (2006) Sunblocking efficiency of various TiO_2-loaded solid lipid nanoparticle formulations. Int J Cosmetic Sci 28: 371–378.

COLIPA (2006) The European Cosmetic Toiletry and Perfumery Association, international sun protection factor (SPF) test method, standardisation mandate assigned to concerning methods for testing efficacy of sunscreen products.

Demirel M, Yazan Y (2000) Katı lipit nanopartiküller (SLN). FABAD J Pharm Sci 25: 167–179.

Demirel M, Yazan Y, Müller RH, Kılıç F, Bozan B (2001) Formulation and *in vitro-in vivo* evaluation of piribedil solid lipid micro- and nanoparticles. J Microencapsulation 18: 359–371.

Diffey BL, Robson J (1989) A new substrate to mesasure sunscreen protection factors throughout the ultraviolet spectrum. J Soc Cosmet Chem 40: 127–133.

El-Gibaly I, Abdel-Ghaffar SK (2005) Effect of hexacosanol on the characteristics of novel sustained-release allopurinol solid lipospheres (SLS): factorial design application and product evaluation. Int J Pharm 294: 33–51.

Freitas C, Lucks JS, Müller RH (1995) Effect of storage conditions on long-term stability of "solid lipid nanoparticles" (SLN) in aqueous dispersion. Proc. 1st World Meeting APGI/APV, Budapest.

Herzog B, Mongiat S, Quass K, Deshayes C (2004) Prediction of sun protection factors and UVA parameters of sunscreens by using a calibrated step film model. J Pharm Sci 93: 1780–1795.

ICH Topic Q2B (1996) Validation of analytical procedures: Methodology. The European Agency for the evaluation of medicinal products. CPMP/ICH/281/95, Step 4, Consensus Guideline.

Kaş HS (2004) Partikül büyüklüğü ve partikül büyüklük dağılımı. In: Gürsoy AZ, editor. Farmasötik Teknoloji: Temel konular ve dozaj şekilleri. İstanbul: Kontrollü Salım Sistemleri Derneği, Piksel Bilişim Matbaacılık Ltd Şti, pp. 69–84.

Kullavanijaya P, Lim HW (2005) Photoprotection. J Am Acad Dermatol 52: 937–958.

Levy SB (2009) UV filters. In: Barel AO, Paye M, Maibach HI (eds.) Handbook of cosmetic science and technology, third edition. New York: Marcel Dekker Inc, pp. 311–321.

Müller RH, Heinemann S (1993) Fat emulsions for parenteral nutrition II: characterisation and physical long-term stability of Lipofundin MCT/LCT. Clinical Nutrition 12: 298–309.

Müller RH, Mäder K, Gohla S (2000) Solid lipid nanoparticles (SLN) for controlled drug delivery - a review of the state of the art. Eur J Pharm Biopharm50: 161–177.

Poiger T, Buser H, Balmer ME, Bergqvist P, Müller MD (2004) Occurrence of UV filter compounds from sunscreens in surface waters: regional mass balance in two Swiss lakes. Chemosphere 55: 951–963.

Salvador A, Chisvert A. Sunscreen analysis, a critical survey on UV filters determination (2005) Anal Chim Acta 537: 1–14.

Scalia S, Mezzena M (2009) Incorporation in lipid microparticles of the UVA filter, butyl methoxydibenzoylmethane combined with the UVB filter, octocrylene: effect on photostability. AAPS PharmSciTech 10: 384–390.

Simeoni S, Tursilli R, Bianchi A, Scalia S (2005) Assay of common sunscreen agents in suncare products by high-performance liquid chromatography on a cyanopropyl-bonded silica column. J Pharm Biomed Anal 38: 250–255.

Takka S, Acartürk F, Ağabeyoğlu İ, Çelebi N, Değim T, Değim Z. Önformülasyon (2007) In: Acartürk F, Ağabeyoğlu İ, Çelebi N, Değim T, Değim Z, Doğanay T, Takka S, Tırnaksız F (eds.) Modern Farmasötik Teknoloji. Ankara: Türk Eczacıları Birliği Eczacılık Akademisi Yayını, Fersa Matbaacılık Ltd Şti, pp. 119–140.

Wissing SA, Müller RH (2001) A novel sunscreen system based on tocopherol acetate incorporated into solid lipid nanoparticles. Int J Cosmetic Sci 23: 233–243.

Wissing SA, Müller RH (2003) Cosmetic applications for solid lipid nanoparticles (SLN). Int J Pharm 254: 65–68.

Wissing SA, Kayserb O, Müller RH (2004) Solid lipid nanoparticles for parenteral drug delivery. Adv Drug Delivery Rev 56: 1257–1272.